WELDABILITY COMPARISON BETWEEN CONVENTIONAL C-MN AND LOWER MN+NB (ULNB) STRUCTURAL STEELS*

Francisco Julião Fuinhas Alves[1]
Antonio Augusto Gorni[2]
Valdeci Paula Alvarenga[3]
Luana Alice de Souza[4]
Paulo Haddad[5]
Celso Custódio Riechelmann[6]

Abstract
In recent years, a new alloy design for hot rolled structural steels was proposed, completely replacing the manganese added with niobium micro-additions, keeping the same mechanical characteristics, but providing advantages in terms of internal quality, cost and carbon footprint. The reduction in carbon equivalent resulting from the no addition of manganese content suggests that the weldability of this new steel should also be improved. However, to be sure of this fact, this work was developed, with the objective to characterize in detail the welded joints of these two types of steel, both from a microstructural and mechanical point of view. The results obtained showed that, as a matter of fact, these steels can also be considered equivalent from the point of view of weldability.
Keywords: Structural Steel; Weldability; Nb Microalloying; Mechanical Properties.

[1] *Metallurgical Engineer, Metallurgical Department, Aperam South America, Timóteo, Minas Gerais, Brazil.*
[2] *PhD, MSc, Materials Engineer, Independent Metallurgical Consultant, São Vicente, São Paulo, Brazil.*
[3] *MSc., Metallurgical Engineer, Specialist Engineer, Metallurgical Department, Aperam South America, Timóteo, Minas Gerais, Brazil.*
[4] *Mechanical Engineering, Technical Assistance and Market Development Department, Aperam South America, São Paulo, São Paulo, Brazil.*
[5] *M.Eng., Metallurgical Engineer, CBMM, São Paulo, São Paulo, Brazil.*
[6] *Metallurgical Engineer, Business Analyst Carbon Steels, Commercial Department, Aperam South America, São Paulo, São Paulo, Brazil.*

** Technical contribution to the 59th Seminário de Laminação, Conformação de Metais e Produtos,part of the ABM Week 8th edition, September 3rd-5th, 2024, São Paulo, SP, Brazil.*

1 INTRODUCTION

The first reference proposing the complete replacement of manganese by niobium in low-carbon hot rolled structural steels was published about twenty years ago [1]. This new alloy design (ULNb steel) has been considered again in recent years due to fluctuations in the price of FeMn and, in the last years, has been successfully implemented in several mills [2-4], including Aperam South America. This new approach, in addition to being able to provide a reduction in the cost of steel, allows that the mechanical properties of the final product are kept but having a microstructure with lower degree of segregation and banding, as well good potential for cost reduction, simplification of liquid steel refining and, most likely, decrease of the carbon footprint when compared to conventional alloys.
It can be predicted that the weldability of this new steel should be better than the conventional alloy (CMn steel), as its lower manganese content will result in a reduction in its equivalent carbon value. However, it is interesting to make a real comparison between the weldability of both two alloys (CMn and ULNb), so that this previous theoretical prediction can be confirmed.
So, the aim of this work was to evaluate the weldability of both steels, CMn and ULNb, under a set of predefined conditions, in order to check eventual differences between their welding performance.

2 DEVELOPMENT

2.1 Experimental Procedure

The steels tested were produced to satisfy the requirements of the SAE 1012/ASTM A36 standards. The samples necessary to the weldability experiments were extracted from hot coils produced in the Steckel mill of Aperam South America, in Timóteo, Brazil. The chemical composition ranges of both steels can be seen in Table 1: the CMn conventional steel, alloy adopted for this product up to now, and the so called ULNb steel, where manganese amount was reduced to residual values and completely replaced by niobium.

TABLE 1: Chemical compositions of both steels studied in this work.

Steel	C [%]	Mn [%]	Nb [%]	Ceq [%]
CMn	0.10 – 0.15	0.30 – 0.60	-	0.15 – 0.25
ULNb	0.10 – 0.15	-	0.008 - 0.015	0.12 – 0.18

The welding experiments described in this paper were carried out at SENAI – Ipatinga [5]. Table 2 shows the experimental planning adopted in this work. As can be seen, there are two types of welded joints: similar, made between the same steels, and dissimilar, between the two different steels. The welding joints were made using an electric arc with shielding gas (GMAW, Gas Metal Arc Welding), using active shielding gas (MAG), composed of a mixture of 92% Argon and 8% CO_2. Filler metal ER70 was used, in accordance with AWS Standard A5.18-2017 [6], with a diameter of 1 mm.

Three levels of welding energy were chosen; the specified process parameters are also included in Table 2.
Macro- and microstructures were revealed using Nital 2% etching of polished samples. The methodology used to identify the HAZ regions in order to measure their width was the comparison of photomicrographs obtained in the analysis, with the start and end regions of the HAZ being determined as described in [7].

Table 2: Proposed welding joints and their specified process parameters.

S	Welding Condition	Tension [V]	Current [A]	Speed [cm/min]	Welding Energy [J/cm]
1	CMn x CMn	20.8	140	23	7.60 (High)
2	ULNb x ULNb	20.8	140	23	
3	CMn x ULNb	20.8	140	23	
4	CMn x CMn	22.4	148	32	6.20 (Standard)
5	ULNb x ULNb	22.4	148	32	
6	CMn x ULNb	22.4	148	32	
7	CMn x CMn	20.8	132	33	5.00 (Low)
8	ULNb x ULNb	20.8	133	33	
9	CMn x ULNb	20.8	132	33	

S: Sample

The preparation of the specimens for mechanical tests included grinding of the samples, aiming to remove regions of lack of fusion in the welded joints. These tests comprised Vickers hardness, tensile, Charpy impact and bending tests. Thickness of the specimens for tensile and Charpy tests was 2.0 mm. Vickers hardness profiles were measured using 1 kg load, three indentations in HAZ left half, fusion zone and HAZ right half, respectively. Tensile tests were carried out on all samples of welded joints, with three tensile tests being carried out for each condition; the welding region was centered on the specimen. Charpy impact tests were carried out in the HAZ region and only in similar joints, at temperatures of -48°C, -20°C, 23°C and 50°C. The guided bending tests at 180° were performed in the face region and in the root region in all welded joints.

2.2 Results and Discussion

Figures 1 to 3 show the aspects observed in the macrographic analysis of the welded joints, respectively using high, standard and low welding energy. All welded joints showed a homogeneous aspect and soundness. However, the similar joints of CMn steel showed incomplete root penetration for all welding energy levels. The intensity of the defect was lower for the joint welded with high energy.
The HAZ microstructures of the welded joints using high energy, samples 1 to 3, were composed of acicular and allotriomorphic ferrite plus pearlite, both for similar and dissimilar joints. In the case of the HAZ of the welded joints made with standard energy, all microstructures were similar to the case of the welded joints with high energy, but they possibly include bainite. An identical situation was observed for the HAZ of the welded joints made with low energy, except in the case of the sample 7, a similar joint between CMn steel, were no bainite was identified. The microstructures obtained here are compatible with those available in the literature [8]. It must be noted that bainite apparently was formed in the welded joints using standard or low energy, whose

cooling rates were lower. However, it would be necessary to analyze such microstructures using electronic microscopy to confirm the formation of bainite, as the resolution of optical microscopy was not enough to fully confirm the presence of this constituent. Finally, there were no significant differences between the HAZ microstructures between CMn and ULNb steels.

(Sample 1) CMn x CMn (Sample 2) ULNb x ULNb (Sample 3) CMn x ULNb

Figure 1: Macrographs of the welded joints made with high welding energy.

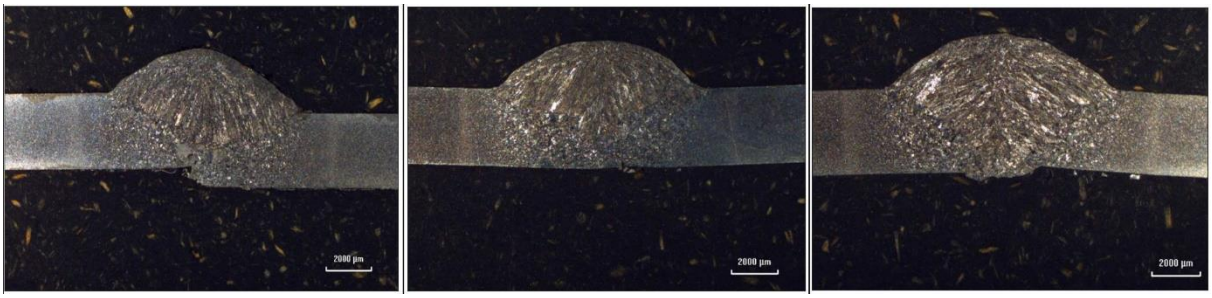

(Sample 4) CMn x CMn (Sample 5) ULNb x ULNb (Sample 6) CMn x ULNb

Figure 2: Macrographs of the welded joints made with standard energy.

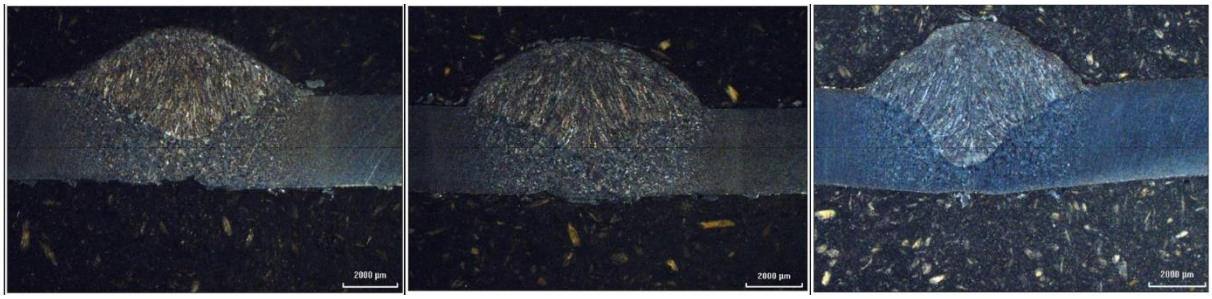

(Sample 7) CMn x CMn (Sample 8) ULNb x ULNb (Sample 9) CMn x ULNb

Figure 3: Macrographs of the welded joints made with low energy.

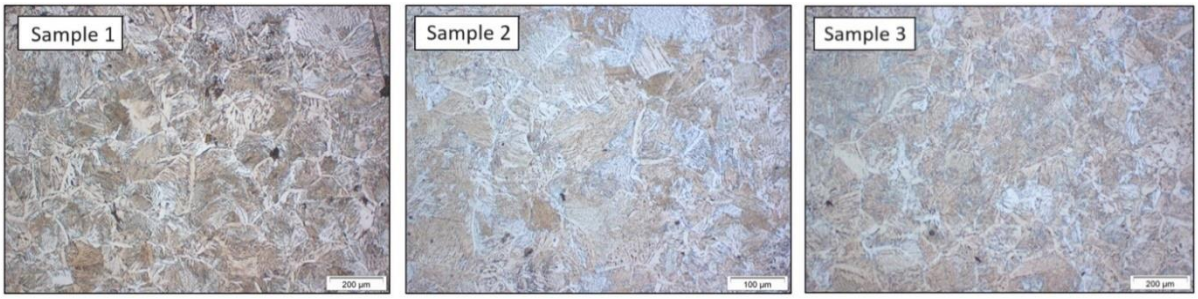

Figure 4: HAZ microstructures of the welding joints using high energy – samples 1, 2 and 3. Nital etching, 100 x magnification.

The average values of the HAZ widths are presented in Table 3. This data shows that there is an increase in the HAZ width as the welding energy used is higher. Variations in the width of the HAZ were observed in both alloys, including when the CMn steel was welded with the ULNb steel.

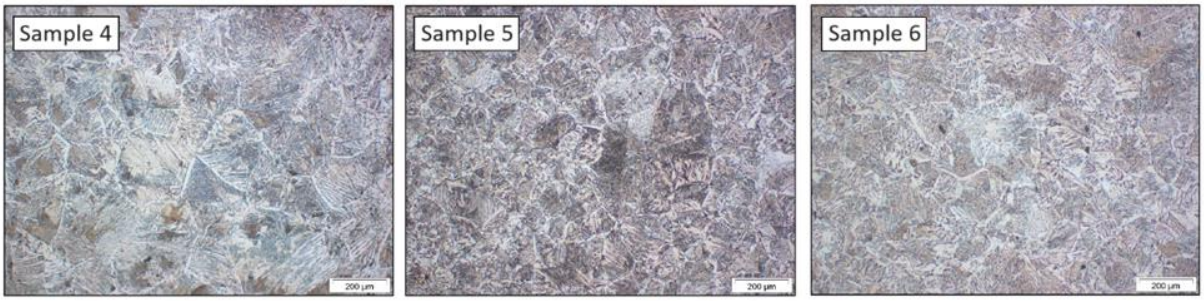

Figure 5: HAZ microstructures of the welding joints using standard energy – samples 4, 5 and 6. Nital etching, 100 x magnification.

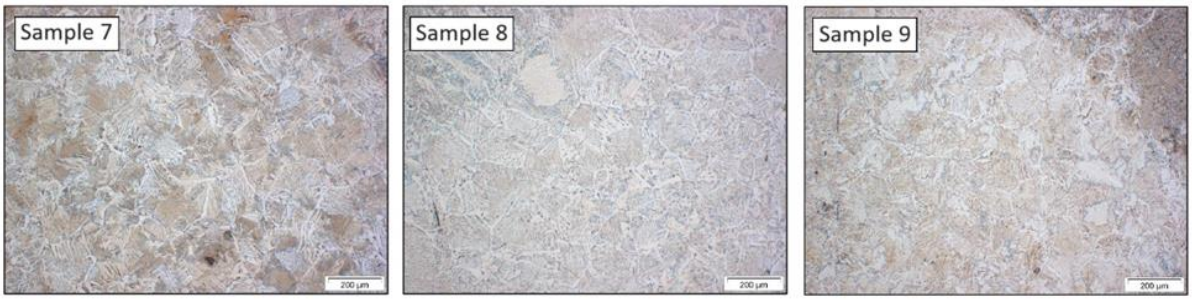

Figure 6: HAZ microstructures of the welding joints using low energy – samples 7, 8 and 9. Nital etching, 100 x magnification.

Table 3. HAZ widths measured at welded joints.

Joined Steels	High Energy			Standard Energy			Low Energy		
	S	HAZ Width (left half) [mm]	HAZ Width (right half) [mm]	S	HAZ Width (left half) [mm]	HAZ Width (right half) [mm]	S	HAZ Width (left half) [mm]	HAZ Width (right half) [mm]
CMn x CMn	1	2.000	1.840	4	1.837	1.674	7	1.314	1.266
ULNb x ULNb	2	2.122	1.902	5	1.726	1.596	8	1.326	1.205
CMn x ULNb	3	2.030	1.713	6	1.480	1.784	9	1.474	1.132

S: Sample

According to the HAZ width measurements, it was also possible to observe that there were no significant differences between the HAZ regions formed in the two different steels. In this way, it was possible to conclude that both alloys (CMn and ULNb) had a similar behavior with regard to the HAZ width in the three energy conditions used in this work.

The laboratory characterization of the welded samples also included microhardness analysis. Microhardness results are presented in Figure 7, for the HAZ (left half), fusion zone and HAZ (right half) regions for high energy, standard energy and low energy welding conditions, respectively.

Some conclusions can be drawn from these results. In the high welding energy condition, HAZ (right half) regions of sample 1 (CMn x CMn) showed higher hardness values, when compared to samples 2 (ULNb x ULNb) and 3 (CMn x ULNb). In the standard welding energy condition, sample 5 (ULNb x ULNb) presented higher hardness values when compared to samples 4 (CMn x CMn) and 6 (CMn x ULNb).The average hardness value of the HAZ(right half) region found in sample 5 was around

13% higher than observed in samples 4 and 6. In the low welding energy condition, the hardness values showed smaller variations in samples 7 (CMn x CMn), 8 (ULNb x ULNb) and 9 (CMn x ULNb), when compared to the previous samples, with the exception of the hardness value of HAZ (right half) of sample 7, which was around 9% below the values of Samples 8 and 9.

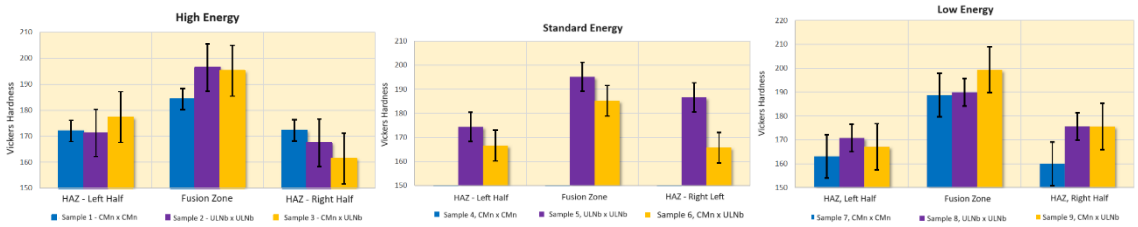

(a) (b) (c)

Figure 7: Vickers hardness measured at both halves of HAZ and in the fusion zone for all welded joints.

In general, the filler metal region (or fusion zone) presented higher hardness values than the HAZ regions. This behavior was observed in all samples. The hardness values of Samples 1 to 9 showed a small variation in results, except for the HAZ (right half) value found in samples 5 and 7. However, the variations in values observed in these samples are within the hardness ranges expected for their respective phases (ferrite and pearlite). Therefore, it can be concluded that no significant differences in hardness were found between the samples welded in the different CMn and ULNb alloys, as well as in the different welding energies used.

Table 4 shows the results got in the tensile tests of all welded joints. All fractures occurred in the base metal, except some cases: in the high energy case, fracture occurred in the weld region in one test of samples 2 (ULNb x ULNb) and 3 (CMn ULNb); in this last sample, fractures in base metal occurred in the side of ULNb steel. All standard energy welded joints showed fracture in the base metal; in the dissimilar joints, Sample 6 (CMn x ULNb), fracture occurred in the ULNb steel side. Finally, in the case of low energy, fracture occurred in the weld region in the case of Sample 7 (CMn x CMn, two tests) and Sample 8 (ULNb x ULNb, one test); in the dissimilar welded joints, sample 9 (CMn x ULNb), all fractures occurred in the ULNb side of the base metal.

Table 4. Results of tensile tests.

Joined Steels	High Energy				Standard Energy				Low Energy			
	S	YS [MPa]	TS [MPa]	E [%]	S	YS [MPa]	TS [MPa]	E [%]	S	YS [MPa]	TS [MPa]	E [%]
CMn x CMn	1	278	497	15	4	405	487	13	7	399	473	13
ULNb x ULNb	2	262	447	13	5	350	458	15	8	318	451	13
CMn x ULNb	3	344	446	14	6	344	465	16	9	272	449	10

S: Sample; YS: Yield Strength; TS: Tensile Strength; E: Elongation

According to the tensile results, it is possible to observe that the samples that failed in the weld region presented the lowest values of mechanical strength and total elongation. This highlights the negative impact of welding on the mechanical properties of these materials. Most of the fractures of the specimens in the weld region occurred in the samples welded under low energy conditions, suggesting an incomplete fusion between the weld and the material as a possible cause of these ruptures.

The rupture in the weld region, observed in samples with high welding energy, may be related to its greater HAZ width, as evidenced in Table 3. This region is characterized

by a microstructure composed of coarser grains, which may have an impact negative effect on the mechanical properties of the material. However, it is necessary to conduct more tests to further investigate this hypothesis, since rupture in the weld region was only observed in two samples from the high welding energy case. The samples welded with standard welding energy showed the best mechanical strength values, and all samples were ruptured in the base metal region.

Finally, based on the results obtained, it is concluded that the CMn alloy presented a higher mechanical resistance than the ULNb alloy. However, the opposite was observed in relation to the elongation results, where the ULNb alloy obtained higher values. One possible explanation for this fact is the higher value of carbon equivalent for CMn steel, as shown in Table 1.

The results of Charpy impact energy of similar welded joints (CMn x CMn and ULNb x ULNb) can be seen in Figure 8. Based on the results obtained, a tendency towards a decrease in the impact absorbed energy values of the welded samples under high energy conditions and standard energy at a temperature of -48 °C was observed. However, this behavior was not observed in the samples welded in the low energy condition, except for the result obtained in one measurement of Sample 7. Apparently, the low value found, far below all other energy values found, appears to be a sample that there was a lack of fusion between the bead and the material. To confirm this hypothesis, other analyzes need to be carried out under this condition.

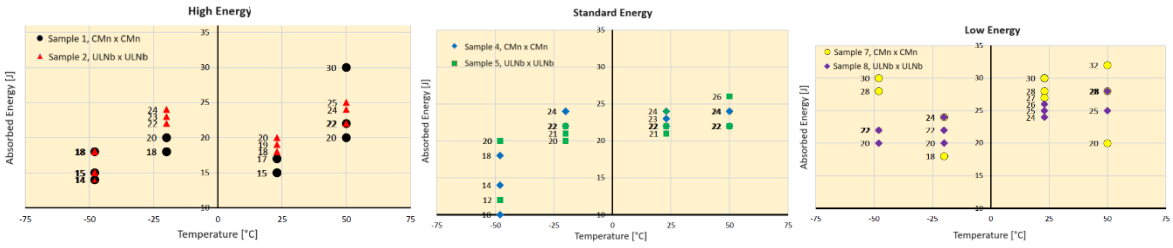

(a) (b) (c)

Figure 8: Charpy impact energy for welded similar joints.

The samples subjected to low welding energy conditions showed the largest standard deviations compared to the other sets, indicating greater variations in the results. However, these cases presented the highest values of impact energy absorption capacity.

The Charpy results got from the CMn and ULNb samples showed only slightly variations in all welding conditions and temperatures used in the tests, with the average energy absorption values showing close values. In this way, one can find that there were no significant differences between the two steels analyzed in the Charpy test.

The results got in the guided bending tests at 180° showed that only the samples welded at low energy showed cracks during bending, specifically in the root region. This weld opening in the root region appears to be related to the lack of complete fusion between the weld and the material. The CMn and ULNb steels showed better results in the standard welding energy condition. The two alloys did not show differences in behavior between them during the bending test.

3 CONCLUSION

Based on the study carried out, from the welding of samples of CMn and ULNb steels under the conditions described here, and subsequent characterization tests, it can be concluded that:

- According to macrographic analysis, samples welded in the low energy condition were the most impacted by the occurrence of lack of penetration in the weld root region;
- In general, samples presented a weld with a homogeneous appearance, good compatibility with the filler metal and absence of discontinuities, except for sample 1 (CMn x CMn, high energy) which presented small regions with porosity;
- The microstructural formations present in the HAZ off welded samples presented basically the same constituents, with no significant differentiation between the CMn and ULNb steels. It was also possible to verify, according to the HAZ width measurements, that there are no significant differences between the HAZs formed in the two different alloys;
- Microhardness analyses, carried out in the HAZ left half, fusion zone and HAZ right half regions, allowed to verify that the fusion zone region presented higher hardness values than the HAZ regions;
- Still according to microhardness analysis, it was observed that the variations in sample values are within the hardness ranges of their microstructural constituents (ferrite and pearlite). Therefore, it can be concluded that no significant differences in hardness were found between the samples welded in the different CMn and ULNb steels, as well as in the different welding energies used;
- Based on the tensile test results, it was possible to verify that the samples welded with standard welding energy presented the best strength values. It can also be concluded that the CMn alloy presented higher strength values than the ULNb alloy. However, the opposite was observed in relation to the elongation results, where the ULNb alloy obtained higher values. These differences could be attributed to the higher value of carbon equivalent of the CMn steel.
- According to the Charpy results got in this work, it was possible to identify a decreasing trend in the absorbed energy values of the welded samples under high and standard energy conditions at a temperature of -48 °C;
- The absorbed energy values of the CMn and ULNb steels showed only a slight variation in all welding conditions and at the temperatures used in the test. In this way, it can be seen that there were no significant differences between the two alloys analyzed in the Charpy test;
- According to the results got in the 180° guided bending tests, the welded joints of both CMn and ULNb steels, using standard energy condition, showed no discontinuities. The two alloys did not show differences in mechanical performance between them during this test.

Therefore, in the present study, no significant differences were observed in the weldability of the two alloys analyzed, that is, CMn and ULNb steels. It was also possible to identify that the use of standard or high energy are the best welding condition for these materials.

Acknowledgments

The authors would like to thank ASA and CBMM for their support during the development of this work and the permission to publish it.

.

REFERENCES

1 YD Morozov, AM Stepashin, SV Aleksandrov. Effect of Manganese and Niobium and Rolling Conditions on the Properties of Low-Alloy Steel. Metallurgist, 2002,46(5-6): 152-156.
2 J Patel. Ultra-Low Niobium (ULNb) Alloying Design Solution for Commodity Grade Structural Steels. Materials Today: Proceedings, 67, 2022, 523-530.
3 AA Gorni, MA Rebellato. Partial Replacement of Manganese by Niobium in Low Carbon Structural Steels. 57th Seminar on Rolling and Metal Forming, Brazilian Association of Metallurgy, Materials and Mining, São Paulo, 2022, 15 p.
4 DDN Guzela, P Haddad, AA Gorni. Benefits for BOF/EAF Steel Plant Resulting from the Partial Substitution of Manganese by Small Additions of Niobium. CONAC 2023 – Steel Industry Congress and Exposition, AIST-Mexico, Monterrey, 2023, 13 p.
5 AS Winther. Estudo Comparativo de Soldabilidade das Ligas P012K e P012W. Relatório Técnico, SENAI Ipatinga - Rinaldo Campos Soares, Julho 2023, 51 p.
6 Specification for Carbon Steel Electrodes and Rods for Gas Shielded Arc Welding. American Welding Society, Miami, 2017.
7 H Colpaert. Metalografia dos Produtos Siderúrgicos Comuns. Editora Blucher, São Paulo, 2008, 652 p.
8 ACS Silva. Caracterização Microestrutural de Juntas Soldadas de Aço ASTM A-1018 Produzidas por Soldagem Helicoidal em Campo. Dissertação de Mestrado, Universidade Federal de Pernambuco, Recife, 2017, 102 p.